Acta Mech 199, 209–216 (2008)
DOI 10.1007/s00707-007-0533-x
Printed in The Netherlands

Acta Mechanica

Porous media convection between vertical walls: continuum of solutions from capped to open ends

P. D. Weidman[1], A. Medina[2]

[1] Department of Mechanical Engineering, University of Colorado, Boulder, CO, USA
[2] Sección de Estudios de Posgrado e Investigación, ESIME-UPA-IPN, Mexico City, Mexico

Received 18 June 2007; Accepted 22 October 2007; Published online 4 February 2008

Summary. Natural convection in a vertical slot filled with a fluid-saturated porous medium modeled by the Brinkman equation is considered. A continuum of solutions are found from capped to open ends in fully-developed two-dimensional flow. This brings to flow in a porous media some aspects of the Newtonian *conduction regime* results of Bühler (Heat Mass Transf. 39: 631, 2003) and the *convection regime* results of Weidman (Heat Mass Transf. 43: 103, 2006). The Brinkman model, valid for sufficiently large porosity and governed by parameter α, allows one to connect Bühler's *conduction regime* flow at low α to a near-Darcy *convection regime* boundary-layer flow at high α.

1 Introduction

Natural convection in fluid-saturated porous media abounds in nature and industrial applications which include ground water movement, oil and gas recovery, catalytic reactors and thermal insulation [1], [2]. The Darcy equation is used to model the low percolation velocity flows, but cannot account for frictional effects at solid boundaries. The Brinkman equation, on the other hand, does include sidewall viscous effects and will be used as the basis of the present investigation. As pointed out in [2], this requires that the porosity ϕ of the medium is sufficiently large: typically $\phi > 0.8$.

Not long ago, Bühler [3] presented a family of solutions for natural convection of a clear fluid in the *conduction regime*. Subsequently Weidman [4] and Magyari [5] extended this work to encompass Newtonian flow of a clear fluid in the *convection regime*. The present paper is one possible extension of these studies to flow in a fluid-saturated porous medium. Our choice using the Brinkman equation permits a comparison of results for the limiting cases of permeability K; the limit $K \to 0$ gives Darcy flow and the limit $K \to \infty$ gives a form of the Navier–Stokes equations. The stable laminar two-dimensional flow in a porous medium confined between parallel vertical walls is considered in this context. For cavity of height l and gap width d we define the cavity aspect ratio $A = l/d$. For $A \gg 1$, it may be accurately assumed that the flow is rectilinear and fully-developed

Correspondence: P. D. Weidman, Department of Mechanical Engineering, University of Colorado, Boulder, CO 80309, USA
e-mail: weidman@colorado.edu

away from capped or open ends; near capped ends there must be a recirculation region, whilst near open ends there are developing boundary layers. We are interested in the continuum of solutions bridging these two limiting cases. It is envisioned that an experiment to observe these flows could be obtained by placing porous caps at the top and bottom of the cavity and varying the porosity from that of the medium to that of solid end caps; see Fig. 1.

An important feature of the problem reported by Bühler [3] is that the position of the reference temperature T_0 for calculating the density ρ using the Boussinesq approximation

$$\rho = \rho_0[1 - \gamma(T - T_0)] \tag{1}$$

moves continuously from the center of the gap for a channel with capped ends to the cold wall for an open-ended channel. Similar results occur in the porous medium problem.

The dimensionless governing equations for fully-developed flow in a fluid-saturated porous medium are formulated and solved analytically in Sect. 2. Asymptotic behaviors of results in the clear fluid limit and the Darcy limit are presented in Sect. 3 and a short discussion of results is provided in Sect. 4.

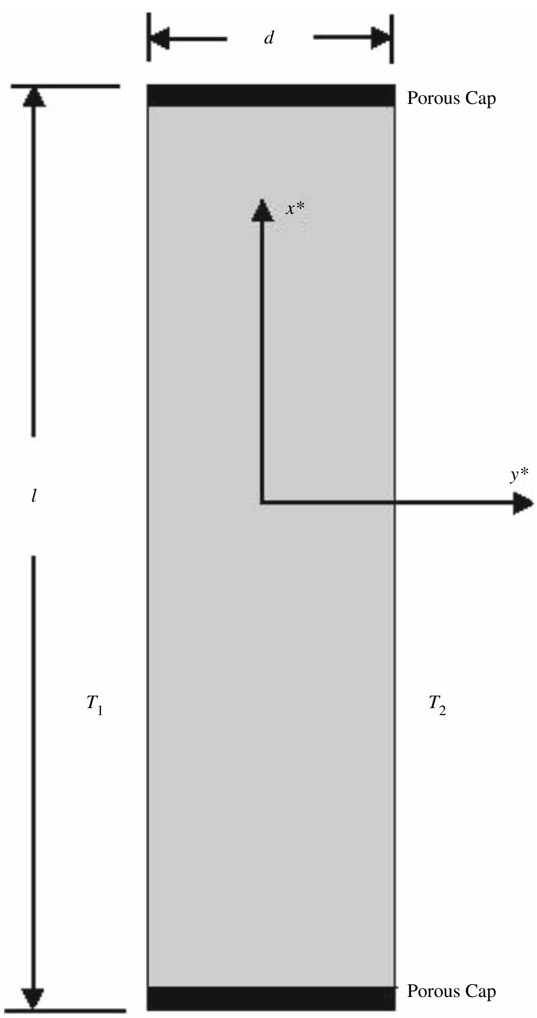

Fig. 1. Schematic drawing of the porous slab and the Cartesian coordinate system

2 Problem formulation and solution

Natural convection flow of a fluid-saturated porous medium between vertical rigid walls in a uniform gravitational field g is considered. The fluid has viscosity μ, thermal expansion coefficient γ, and $\tilde{\mu}$ is the effective viscosity of the fluid-saturated porous matrix. Following [4], we employ a Cartesian coordinate system centered in the gap with x^* directed upwards antiparallel to gravity and y^* the cross-channel coordinate, with respective velocity components (u^*, v^*). The porous end caps shown in Fig. 1 are for illustration purposes only; we do not model the pressure drop across the end caps and only consider the fully-developed flow far from the end caps. The thermal boundary conditions on the vertical walls are noted in Fig. 1 and the velocity conditions are those of impermeablity and no-slip. Without loss of generality, the right wall is taken to be hot relative to the left wall so that $\Delta T = (T_2 - T_1) > 0$. The dimensional governing equations for steady planar motion are the continuity equation, the Brinkman equation, and the energy equation in which the viscous heating term is neglected. Away from the top and bottom ends of the cavity the flow is rectilinear so that $u^* = u^*(y^*), v^* = 0$ in which case continuity is satisfied identically. Assuming no imposed external pressure gradient, the remaining momentum and energy equations are given by

$$\frac{\mu}{K}u^* = -\frac{\partial p}{\partial x^*} + \tilde{\mu}\frac{\partial^2 u^*}{\partial y^{*2}} - \rho g, \tag{2}$$

$$\frac{\partial^2 T}{\partial y^{*2}} = 0. \tag{3}$$

Invoking the Boussinesq approximation (1) into the Brinkman equation (2) yields

$$\begin{aligned}\frac{\mu}{K}u^* &= -\frac{\partial p}{\partial x^*} + \tilde{\mu}\frac{\partial^2 u^*}{\partial y^{*2}} - \rho_0 g + \rho_0 g\gamma(T - T_0)\\ &= \frac{\partial}{\partial x^*}(p + \rho_0 g x^*) + \tilde{\mu}\frac{\partial^2 u^*}{\partial y^{*2}} + \rho_0 g\gamma(T - T_0).\end{aligned} \tag{4}$$

In the asymptotic state of fully-developed *free convection* flow in a long vertical channel, the gradient of the pressure excess $(p + \rho_0\, g\, x^*)$ above the hydrostatic pressure $(-\rho_0\, g\, x^*)$ goes to zero and Eq. (4) becomes

$$\tilde{\mu}\frac{\partial^2 u^*}{\partial y^{*2}} = \frac{\mu}{K}u^* - \rho_0 g\gamma(T - T_0). \tag{5}$$

Scaling y^* with d, the velocity u^* with $\rho_0 g\gamma\, K\Delta T/\mu$ and introducing $\theta = (T - T_0)/\Delta T$, the dimensionless governing equations are

$$u_{yy} - \alpha^2 u = -\alpha^2\theta, \tag{6}$$

$$\theta_{yy} = 0, \tag{7}$$

in which a subcript denotes differentiation with respect to the subscripted variable. The single governing parameter is $\alpha^2 = 1/MDa$, where $M = \tilde{\mu}/\mu$ is the viscosity ratio and $Da = K/d^2$ is the Darcy number. Note that the limit $\alpha \to 0$ gives a clear fluid and the limit $\alpha \to \infty$ gives unmitigated Darcy flow. The no-slip velocity conditions and isothermal wall conditions are, respectively,

$$u(-1/2) = 0, \quad u(1/2) = 0; \qquad \theta(-1/2) = -\theta_0, \quad \theta(1/2) = 1 - \theta_0, \tag{8}$$

wherein the parameter θ_0 measures the continuous cross-channel variation of the reference temperature T_0 used to calculate the density in Eq. (1), namely

$T_0 = T_1 + \theta_0 \Delta T$.

The temperature field satisfying the temperature boundary conditions (8) is simply

$$\theta(y) = y + \left(\frac{1}{2} - \theta_0\right). \tag{9}$$

Inserting Eq. (9) into (6) gives the inhomogenous ordinary differential equation for the velocity field, the general solution of which is readily determined to be

$$u(y) = A \cosh \alpha y + B \sinh \alpha y + y + \left(\frac{1}{2} - \theta_0\right). \tag{10}$$

Application of the velocity boundary conditons in Eq. (6) gives the desired solution

$$u(y) = y + \left(\frac{1}{2} - \theta_0\right)\left(1 - \frac{\cosh \alpha y}{\cosh(\alpha/2)}\right) - \frac{1}{2}\frac{\sinh \alpha y}{\sinh(\alpha/2)}. \tag{11}$$

Thus we have a two-parameter family of solutions, depending on both α and θ_0.

Of interest is the normalized planar volume flux $Q = Q^*/(\rho_0 g \gamma K d \Delta T/\mu)$ up the cavity. The only contribution comes from the symmetric portion of the velocity profile which, when integrated across the gap, yields

$$Q = \left(\frac{1}{2} - \theta_0\right)\left(1 - \frac{\tanh(\alpha/2)}{\alpha/2}\right). \tag{12}$$

When $\theta_0 = 1/2$ it is evident that the cavity is closed since $Q = 0$. As θ_0 decreases to $\theta_0 = 0$ the porous end caps tend to the porosity of the fluid-saturated medium. Maximum throughflow occurs at $\theta_0 = 0$ in Eq. (12) which gives

$$Q_{\max} = \left(\frac{1}{2} - \frac{\tanh(\alpha/2)}{\alpha}\right). \tag{13}$$

These results are summarized in Table 1.

As θ_0 decreases from its maximum value $\theta_0 = 1/2$, there comes a value $\theta_0 = (\theta_0)_c$ for incipient reverse flow which occurs on the left, cold wall. The condition for incipient backflow is thus given by

$$\left.\frac{du}{dy}\right|_{y=-\frac{1}{2}} = 0, \tag{14}$$

which gives rise to the equation for the critical value of θ_0, viz.,

$$(\theta_0)_c = \frac{1}{2} + \left(\frac{2 - \alpha \coth(\alpha/2)}{2\alpha \tanh(\alpha/2)}\right). \tag{15}$$

Temperature profiles for six uniformly incremented values of θ_0 are presented in Fig. 2. Velocity profiles for the same six values of θ_0 are given in Figs. 3a–d for the respective values $\alpha = 0.1$, 1.0, 10 and 100. The obvious feature to be observed is the tendency of the profiles toward straight lines as $\alpha \to \infty$ corresponding to pure Darcy flow which allows slip at the vertical walls. Indeed, as expected, the velocity and temperature profiles in the Darcy limit are identical. Plots of the variation

Table 1. Limiting parameter values for capped and open ends

End condition	Flow rate	Reference temperature	Parameter
Capped	$Q = 0$	$T_0 = (T_1 + T_2)/2$	$\theta_0 = 1/2$
Open	$Q = Q_{\max}$	$T_0 = T_1$	$\theta_0 = 0$

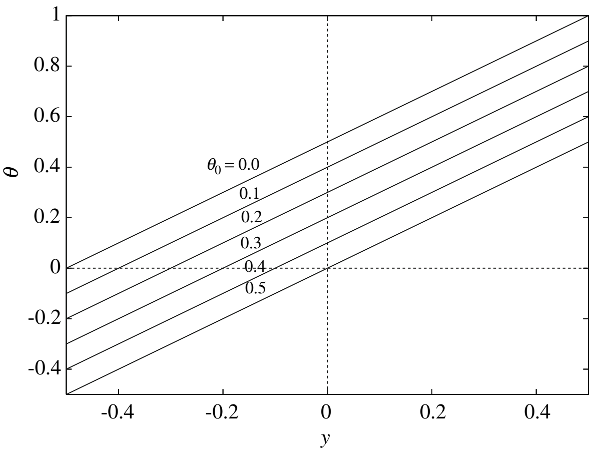

Fig. 2. Temperature profiles for six values of θ_0 spanning capped to open ends

of volume flowrates $Q(\alpha)$ for selected values of θ_0 are presented in Fig. 4, and the critical values $(\theta_0)_c$ for incipient backflow are plotted in Fig. 5.

3 Asymptotic behaviors

Of practical interest is the asymptotic behavior of results in the limit $\alpha \to 0$ corresponding to a clear fluid and in the limit $\alpha \to \infty$ corresponding to Darcy flow. In both cases the temperature distributions across the gap are the same linear profiles (9) dependent only on θ_0.

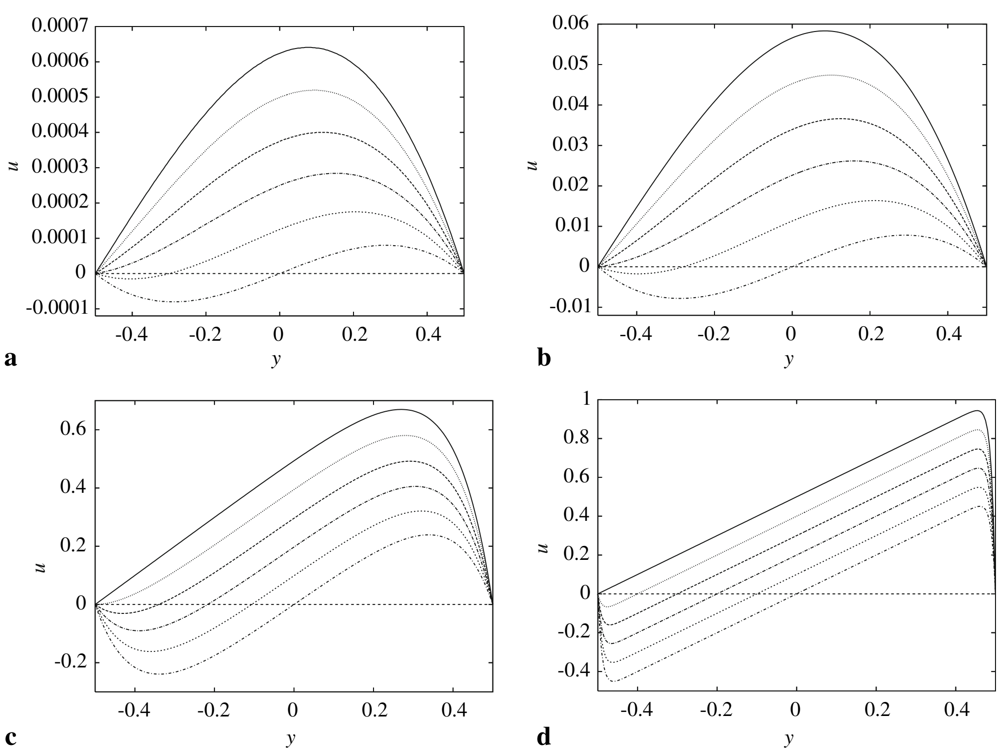

Fig. 3. Velocity profiles spanning capped to open ends for **a** $\alpha = 0.1$, **b** $\alpha = 1.0$, **c** $\alpha = 10.0$ and **d** $\alpha = 100.0$

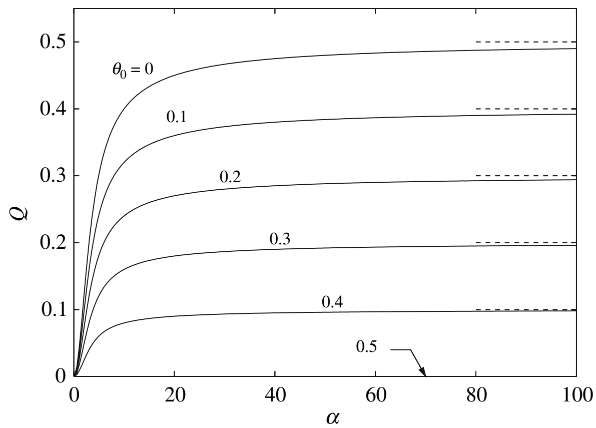

Fig. 4. Dimensionless volume flux Q up the cavity as a function of α for selected values of θ_0. The *horizontal dashed lines* give the asymptotic behaviors as $\alpha \to \infty$ according to Eq. (20)

3.1 The clear fluid limit

In the limit $\alpha \to 0$ the leading behavior of the velocity field is given by

$$u(y) \sim \frac{1}{6}\left(\frac{1}{4} - y^2\right)\left[y + 3\left(\frac{1}{2} - \theta_0\right)\right]\alpha^2 + O(\alpha^4). \quad (16)$$

When properly scaled for a clear fluid in the absence of a porous medium, the leading $O(\alpha^2)$ term is seen to reproduce the results of Bühler [3] which in the present notation is given by Eq. (21) in [4]. Taking the $\alpha \to 0$ limit of the volume flowrate expression in Eq. (12) furnishes the result

$$Q \sim \left(\frac{1}{2} - \theta_0\right)\frac{\alpha^2}{12} + O(\alpha^4). \quad (17)$$

Finally, the $\alpha \to 0$ limit of condition (15) for incipient backflow gives the leading behavior

$$(\theta_0)_c \sim \frac{1}{3} - \frac{\alpha^2}{90} + O(\alpha^4). \quad (18)$$

The above leading behaviors are in agreement with the *conduction regime* results for a clear fluid given in [3]. The low α behavior in (18) is compared with the numerically computed critical values of $(\theta_0)_c$ plotted in Fig. 5.

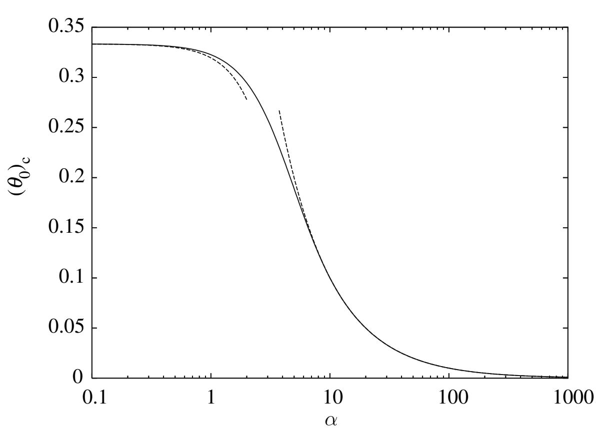

Fig. 5. Critical value of θ_0 for onset of backflow at the cold wall as a function of α. The low and high α asymptotical behaviors given by Eqs. (18) and (21), respectively, are shown as *dashed lines*

3.2 The Darcy limit

In the limit $\alpha \to \infty$ the leading behavior of the velocity field is given in two parts, one for y positive and one for y negative. The results are

$$u(y) \sim \begin{cases} y + \left(\frac{1}{2} - \theta_0\right) - (1 - \theta_0)e^{\alpha(y-1/2)} & y > 0 \\ y + \left(\frac{1}{2} - \theta_0\right) + \theta_0 e^{-\alpha(y+1/2)} & y < 0. \end{cases} \tag{19}$$

Taking the $\alpha \to \infty$ limit of the volume flowrate in Eq. (12) yields

$$Q \sim \left(\frac{1}{2} - \theta_0\right)\left(1 - \frac{2}{\alpha}\right) + O(\alpha^3). \tag{20}$$

Finally, the $\alpha \to \infty$ limit of criterion (15) for incipient backflow is given by

$$(\theta_0)_c \sim \frac{1}{\alpha} + O(\alpha^3). \tag{21}$$

The latter two asymptotic behaviors are plotted for comparsion with the numerically determined results in Figs. 4 and 5.

4 Discussion

Building on the studies of Bühler [3] and Weidman [4] who considered fully-developed natural convection of a Newtonian fluid between vertical walls, spanning end wall conditions from capped to open ends, an analogous problem of fully-developed convection in a fluid-saturated porous medium is presented. Results are obtained using a nondimensional form of the Brinkman equation governed by the single parameter α. While this model of porous media flow is restricted to relatively large porosities, it has the advantage of bridging the gap between Newtonian flow as $\alpha \to 0$ and Darcy flow when $\alpha \to \infty$. The interesting feature of the capped and open end solutions obtained is that the Brinkman model connects, at low α, a *conduction regime* Newtonian flow to, at high α, a near Darcy boundary layer flow. The $\alpha \to \infty$ limit, however, is non-uniform. For α large but finite, the no-slip boundary layer flow described by Eq. (19) accurately gives the velocity profiles plotted in Fig. 3d. For $\alpha \equiv \infty$, on the other hand, the classical Darcy flow with slip at the vertical walls is recovered; in this case the velocity profiles in Fig. 3 become identical to the temperature profiles displayed in Fig. 2, as expected.

Acknowledgements

The authors acknowledge the help of a referee who pointed out a dimensional inconsistency in the derivation of the governing equation.

References

[1] Kaviany, M.: Principles of Heat Transfer in Porous Media. Springer, New York (1991)
[2] Nield, D.A., Bejan, A.: Convection in Porous Media, 3rd edn. Springer, New York (2006)

[3] Bühler, K.: Special solutions of the Boussinesq-equations for free convection flows in a vertical gap. Heat Mass Transfer **39**, 631–638 (2003)

[4] Weidman, P.D.: Convection regime flow in a vertical slot: continuum of solutions from capped to open ends. Heat Mass Transfer **43**, 103–109 (2006)

[5] Magyari, E.: Normal mode analysis of the fully developed free convection flow in a vertical slot with open to capped ends. Heat Mass Transfer **43**, 827–832 (2007)